ACS OMEGA

Article

Cite This: ACS Omega 2018, 3, 18990−18999

http://pubs.acs.org/journal/acsodf

Cationic Gemini Surfactants with a Bipyridyl Spacer as Corrosion Inhibitors for Carbon Steel

Liwei Feng,[†] Chengxian Yin,[*,‡] Huali Zhang,[§] Yufei Li,[§] Xuehua Song,[†] Qibin Chen,[*,†] and Honglai Liu[†]

[†]State Key Laboratory of Chemical Engineering, School of Chemistry & Molecular Engineering, East China University of Science and Technology, Shanghai 200237, P. R. China

[‡]State Key Laboratory for Performance and Structure Safety of Petroleum Tubular Goods and Equipment Materials, Xi'an, Shanxi 710065, P. R. China

[§]Engineering and Technology Research Institute of Southwest Oil & Gas Field Company, PetroChina, Chengdu, Sichuan 610017, P. R. China

Supporting Information

ABSTRACT: In this work, cationic Gemini surfactants with different alkyl chain lengths (n = 8, 10, and 12) and a bipyridyl spacer were synthesized and tested as corrosion inhibitors for carbon steel in 1 M HCl solution. The corrosion inhibition efficiency was determined by weight loss measurement, potentiodynamic polarization, and electrochemical impedance spectroscopy. Results showed that such three inhibitors could effectively inhibit the corrosion of carbon steel in 1 M HCl solution, especially at their low concentrations, while the carbon chain length of Geminis used played a negligible role in the inhibition efficiency. Scanning electron microscopy/energy dispersive X-ray analysis observations demonstrated the formation of a protective inhibitor layer on the carbon steel surface. Additionally, the adsorption of the inhibitor molecules on the carbon steel surface was found to obey the Langmuir isotherm.

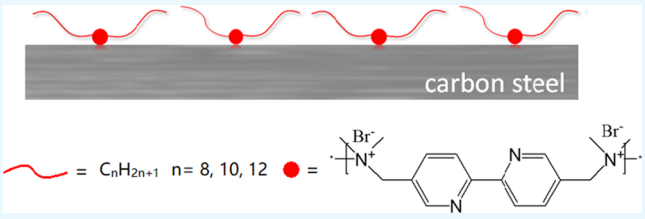

1. INTRODUCTION

Carbon steel, as a main construction material, is widely used in many engineering fields, such as the oil and gas transmission, power production, desalination, petroleum, food, and chemical and electrochemical industries because of its low cost, good mechanical properties, and easy availability for fabrication of vessels.[1−3] However, carbon steel is highly sensitive to corrode in different aggressive media, especially in the acidic environment.[4,5] Unfortunately, acid solutions are widely used for industrial descaling, cleaning, oil well acidification, and in petrochemical processes.[6] To date, several methods have accordingly been employed to control these corrosion processes. In this regard, the use of corrosion inhibitors is the most practical method due to many advantages, such as economy, high efficiency, environmental friendliness, and wide applicability in various fields.[7,8]

In general, the inhibitors can adsorb onto a metal surface through the so-called physisorption and/or chemisorption and thus form a protective barrier layer against metal corrosion in aggressive environments.[9] Here, the former involves electrostatic attraction between charged metal surface and oppositely charged inhibitors, while the latter requires fulfilling charge sharing or charge transfer of lone-pair and/or π electrons from conjugated moieties of inhibitor molecules to empty d-orbitals of the metal surface. Besides, as for the aromatic systems, the π^* orbital can also accept the electrons of d-orbital of iron to form feedback bonds, thereby producing more than one center of chemical adsorption action.[10] As a result, most organic compounds that were used as corrosion inhibitors can be adsorbed on metal surface via heteroatoms, such as nitrogen, sulfur, oxygen, and phosphorus, multiple bonds or aromatic rings, and oppositely charged groups relative to the charged metal surface, like quaternary ammonium salts.[11] A typical class of organic inhibitors is surfactants due to the special amphiphilicity of their molecular structures, which can be readily synthesized with low cost and have high effectiveness and efficiency for the inhibiting corrosion.[11−13] Over the last 3 decades, Gemini surfactants have aroused remarkable interest in the interfacial and colloid field. Gemini surfactants are composed of two amphiphilic moieties linked by a spacer group at or near two head groups,[14,15] affording a great number of unique performances, such as lower critical micelle concentrations (CMCs) and C_{20} (the surfactant concentration at which the surface tension is decreased by 20 mN m^{-1}), better solubilizing abilities, greater wetting, foaming and lime-soap dispersing properties, and stronger biological activities, compared to conventional single-tail-and-single-head surfactants.[16] More recently, an increasing concern has been focused

Received: October 31, 2018
Accepted: December 21, 2018
Published: December 31, 2018

DOI: 10.1021/acsomega.8b03043
ACS Omega 2018, 3, 18990−18999

on the investigation of the inhibition behavior of Gemini surfactants in various aggressive media, most of which have exhibited high effectiveness exceeding 90%.[17] In particular, the roles that the nature of spacers and the length of alkyl chains in Gemini molecules play in the inhibitive performances have extensively been investigated to date.[18−20] However, most of such Gemini surfactants contained single functional groups[20,21] or a variety of combinations of double functional groups[22−24] among heteroatoms, conjugated and charged head groups, whereas few of them included these triple functional groups simultaneously.[18,25] In principle, the effectiveness of inhibitors is strongly related to the formation of their adsorbed layers on the metal surfaces, mainly influenced by the chemical nature and structure of inhibitors and the charge of metal surfaces as well. Therefore, the effect of Gemini surfactants having heteroatoms, aromatic rings, and polar head groups on the inhibitive corrosion remains to be investigated. Also, we noted that the addition of halide ions might promote the inhibition performances of cationic Gemini surfactants,[26−28] and thus its influence on halide ions was explored in this work.

In the present work, our primary goal was 3-fold: (i) to test the effect of Gemini surfactant simultaneously bearing heteroatoms, aromatic rings, and quaternary ammonium head groups on the inhibitive behaviors, (ii) to determine the extent to which the multiple interactions between inhibitors and metal surface influence the inhibitive performances, and (iii) to examine the effect of the addition of halide ions on the enhanced inhibition performances of Gemini surfactants. To address these issues, we designed and synthesized a series of novel cationic Gemini surfactants, 2,2′-bipyridyl-5,5′-dimethylene-bis(*N*,*N*′-dimethylalkylammonium bromide), referred to as *n*-Bpy (here, *n* denotes the carbon atom number of alkyl chains, *n* = 8, 10, and 12), as shown in Chart 1. Herein, *n*-Bpy was selected as corrosion

Chart 1. Chemical Structure of the Synthesized Cationic Gemini Surfactants

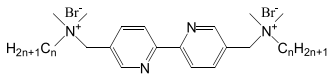

n= 8, 10, 12

inhibitors of carbon steel in 1 M HCl solution. The anticorrosion performance of *n*-Bpys was investigated by weight loss measurements, electrochemical measurements (potentiodynamic polarization and electrochemical impedance spectroscopy), and surface assessment techniques (scanning electron microscopy (SEM)/energy-dispersive X-ray spectroscopy (EDS)). Additionally, 0.1 M potassium iodide as a secondary species was added to the simulated corrosion solution to define the effect between halide ions and *n*-Bpys. Results show that *n*-Bpys exhibit a comparable and even superior inhibition efficiency, especially at low concentration, compared to those reported in previous work.[25,29,30]

2. RESULTS AND DISCUSSION

2.1. Weight Loss Measurements. The inhibition efficiency and corrosion rate, obtained from the weight loss method at different concentrations of *n*-Bpys and in the mixed solution of 10^{-5} M *n*-Bpys plus 0.1 M KI, are summarized in Table 1. The corrosion rate (v) is calculated as follows

$$v = \frac{w_0 - w}{S \times t} \quad (1)$$

Table 1. Corrosion Parameters of *n*-Bpys Obtained from Weight Loss Measurements for Carbon Steel in 1 M HCl

inhibitor	C_{inh}/M	v/mg cm^{-2} h^{-1}	θ	η/%
blank	0	0.168		
8-Bpy	10^{-7}	0.064	0.62	61.9
	10^{-6}	0.036	0.79	78.8
	10^{-5}	0.031	0.82	81.7
	10^{-4}	0.028	0.83	83.4
8-Bpy + 0.1 M KI	10^{-5}	0.012	0.93	92.8
10-Bpy	10^{-7}	0.045	0.73	73.0
	10^{-6}	0.028	0.83	83.4
	10^{-5}	0.023	0.86	86.2
	10^{-4}	0.020	0.88	88.1
10-Bpy + 0.1 M KI	10^{-5}	0.013	0.92	92.3
12-Bpy	10^{-7}	0.132	0.22	21.8
	10^{-6}	0.030	0.82	82.0
	10^{-5}	0.024	0.86	85.8
	10^{-4}	0.019	0.89	88.6
12-Bpy + 0.1 M KI	10^{-5}	0.015	0.91	91.1

where w_0 and w are the weight values without and with *n*-Bpys, respectively, S is the surface area of carbon steel sheet, and t is the immersion time. The inhibition efficiency (η) together with the surface coverage (θ) was calculated according to the following equation

$$\eta = \frac{\nu_0 - \nu}{\nu_0} \times 100\% \quad (2)$$

$$\theta = \frac{\nu_0 - \nu}{\nu_0} \quad (3)$$

where ν_0 and ν are the corrosion rate values in the absence and presence of *n*-Bpys, respectively.

As is apparent, weight loss measurements reveal that the addition of *n*-Bpys suppresses the corrosion process markedly. Two striking features appear: (i) *n*-Bpy exhibits good inhibition efficiencies at low concentrations, e.g., even as low as 10^{-7} M; and (ii) the inhibition efficiency increases with *n*-Bpy concentrations, accompanied with the decreasing corrosion rate, and attains about 83, 88, and 89% for 8-Bpy, 10-Bpy, and 12-Bpy at 10^{-4} M only, respectively. These results suggest that *n*-Bpys are excellent inhibitors, especially at their low concentrations. Additionally, we examined the influence of temperature on the inhibitive performances of 12-Bpy and found that the effect of varying temperature (in a lower-temperature range, <318 K) on the inhibition corrosion efficiency is almost negligible, while the efficiency value is greatly reduced at a higher temperature (338 K) (see Figure S1).

For a compromise among the inhibitor concentration, corrosion rate, and inhibitive efficiency, the concentration of 10^{-5} M appears to be an optimal choice for such three inhibitors. Accordingly, at such an *n*-Bpys concentration (10^{-5} M), we investigated the influence of the addition of iodide ions on the inhibitive performances of iron. Herein, the inhibition efficiency increased by ∼11, 6, and 5% for 8-Bpy, 10-Bpy, and 12-Bpy, respectively, and the percentage of inhibition efficiency reached up to around 93, 92, and 91%, after the addition of iodide ions into 1 M HCl solution with 10^{-5} M *n*-Bpys. This result indicates that introducing iodide ions can improve the value of the inhibition efficiency. Additionally, the variation of inhibition efficiency with inhibitor concentration would be further

DOI: 10.1021/acsomega.8b03043
ACS Omega 2018, 3, 18990−18999

confirmed by the following potentiodynamic polarization and EIS results.

2.2. Potentiodynamic Polarization. Figure 1a reveals the cathodic and anodic polarization curves for the carbon steel in 1 M HCl without and with the addition of different *n*-Bpy concentrations. Herein, only 8-Bpy curves are given, while those of 10-Bpy and 12-Bpy are shown in Figure S2. Obviously, the addition of *n*-Bpys results in shifts in both the cathodic and anodic curves but with different extents, and this inhibition effect becomes more prominent as the *n*-Bpy concentration is increased, evidenced by the fact that both anodic and cathodic current densities gradually decrease with the *n*-Bpy concentrations as a whole. Additionally, Figure 1b depicts the potentiodynamic polarization curves for carbon steel in 10^{-5} M 8-Bpy solution in the absence and presence of 0.1 M KI (those of 10-Bpy and 12-Bpy, see Figure S3). Herein, the corrosion current density decreased sharply in the presence of 0.1 M iodide ions, compared to that in the iodide-free solution.

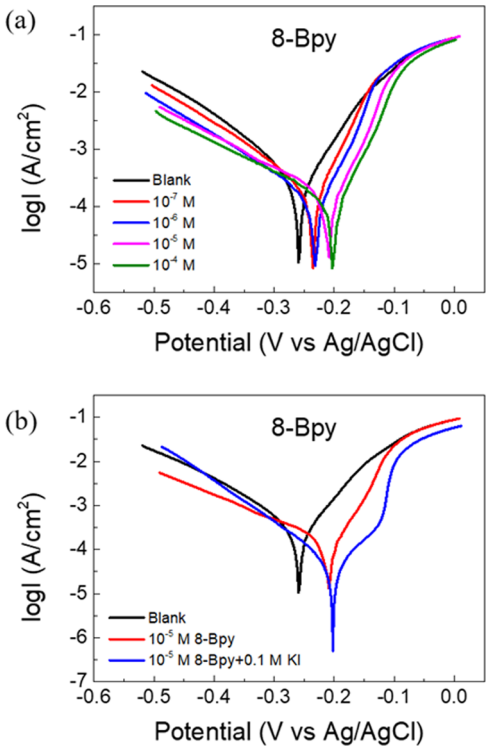

Figure 1. Potentiodynamic polarization curves for carbon steel in 1 M HCl (a) without and with different concentrations of 8-Bpy; (b) blank, blank + 10^{-5} M 8-Bpy and blank + 10^{-5} M 8-Bpy + 0.1 M KI.

The polarization curves displayed a reasonable linear Tafel region in both anodic and cathodic branches. Therefore, to obtain more information about the kinetics of the dissolution process of carbon steel, the related electrochemical parameters, including corrosion potential (E_{corr}), corrosion current density (I_{corr}), anodic Tafel slopes (β_a), cathodic Tafel slopes (β_c), and the inhibition efficiency (η%) values, were determined and compiled in Table 2. The inhibition efficiency (η%) values of the inhibitors were calculated using I_{corr} values as formulated with the following equation

$$\eta = \frac{I_{corr} - I_{inh}}{I_{corr}} \times 100\% \quad (4)$$

where I_{corr} and I_{inh} are uninhibited and inhibited corrosion current densities, respectively, obtained from the extrapolation of cathodic and anodic Tafel lines to the corrosion potential.

Apparently, the addition of *n*-Bpys leads to a sharp reduction in the corrosion current densities (I_{corr}), and moreover, the I_{corr} value further decreases with increasing *n*-Bpy concentration, while the inhibition efficiency increases. Herein, the I_{corr} value shifts from 0.6025 mA cm^{-2} (blank) to 0.1044 mA cm^{-2} (8-Bpy), 0.0913 mA cm^{-2} (10-Bpy), and 0.0795 mA cm^{-2} (12-Bpy), at its concentration of 10^{-7} M alone, whereas their inhibition efficiencies increased separately up to 82.7, 84.8, and 86.8%, respectively. This result suggests that *n*-Bpys show a great inhibition effect even at a low concentration. In particular, the cathodic Tafel slope (β_c) increases with concentrations in the presence of *n*-Bpys, while the anodic slope (β_a) decreases, and meanwhile, the change in β_c is larger than that in β_a, the anodic slope. In addition, no definite tendency in the shift of E_{corr} values is observed as the *n*-Bpy concentration is increased, and the maximum E_{corr} shift is 59 mV. Taken together, the variation in β_c and β_a and the shift in E_{corr} imply that *n*-Bpys behave as mixed-

Table 2. Potentiodynamic Polarization Parameters for Carbon Steel in 1 M HCl in the Absence and Presence of Different Concentrations of *n*-Bpys, and 10^{-5} M *n*-Bpys + 0.1 M KI

inhibitor	C_{inh}/M	E_{corr}/V	I_{corr}/mA cm^{-2}	β_a/V dec^{-1}	β_c/V dec^{-1}	η/%
blank	0	−0.2594	0.6025	0.0660	−0.1500	
8-Bpy	10^{-7}	−0.2353	0.2290	0.0450	−0.1545	62.0
	10^{-6}	−0.2313	0.1349	0.0427	−0.1582	77.6
	10^{-5}	−0.2095	0.1266	0.0420	−0.1815	79.0
	10^{-4}	−0.2019	0.1044	0.0406	−0.1955	82.7
8-Bpy + 0.1 M KI	10^{-5}	−0.2007	0.0426	0.0779	−0.1071	92.9
10-Bpy	10^{-7}	−0.2980	0.2163	0.0511	−0.1519	64.1
	10^{-6}	−0.2802	0.2077	0.0452	−0.1848	65.5
	10^{-5}	−0.2594	0.1323	0.0425	−0.1867	78.0
	10^{-4}	−0.2381	0.0913	0.0382	−0.2309	84.8
10-Bpy + 0.1 M KI	10^{-5}	−0.2486	0.0298	0.0879	−0.1200	95.0
12-Bpy	10^{-7}	−0.2707	0.3083	0.0566	−0.1600	48.8
	10^{-6}	−0.2447	0.1651	0.0397	−0.1693	72.6
	10^{-5}	−0.2071	0.1224	0.0348	−0.2792	79.7
	10^{-4}	−0.2002	0.0795	0.0336	−0.2479	86.8
12-Bpy + 0.1 M KI	10^{-5}	−0.2651	0.0449	0.0964	−0.1651	92.5

DOI: 10.1021/acsomega.8b03043
ACS Omega 2018, 3, 18990−18999

type inhibitors and act on both the hydrogen evolution reaction and metal dissolution, but with a predominant control of the cathodic reaction.[31,32]

We also investigated the influence of adding iodide ion on the inhibitive performances of iron, as mentioned in the previous section. After the addition of KI into 1 M HCl solution with 10^{-5} M *n*-Bpys, the corrosion current density decreases remarkably compared to that in the solution without KI. The inhibition efficiencies increase by ~14, 17, and 13% for 8-Bpy, 10-Bpy, and 12-Bpy, respectively, and correspondingly reach up to around 93, 95, and 92% after the iodide ions are introduced in this system.

2.3. Electrochemical Impedance Spectroscopy (EIS). The EIS technique provides exact and rapid information about the kinetics of the electrode processes and the properties of the metal surface without destroying the adsorbed layer on the metal surface. Figure 2 shows the Nyquist plots (a) and Bode and phase angle plots (b) for carbon steel in 1 M HCl solution without and with different concentrations of 8-Bpy. Similar plots of the other two *n*-Bpys, 10-Bpy and 12-Bpy, are shown in Figures S4 and S5. Three key issues can be obtained from Figure 2a: (i) all of the obtained impedance spectra exhibit a single capacitive loop with a progressively incremental diameter with *n*-Bpy concentrations, which suggests that the corrosion of carbon steel in both uninhibited and inhibited 1 M HCl is usually related to the double-layer behavior and mostly controlled by a charge-transfer process;[33] (ii) the addition of *n*-Bpys leads to stronger dispersion effects, compared to the blank sample, which can be attributed to the resistance of the adsorbed *n*-Bpy molecules;[34] and (iii) all semicircles display a slightly depressed nature with a center under the real axis, attributed to the dispersion in frequency due to different physical phenomena, such as inhomogeneity and roughness of the solid during corrosion.[33] Accordingly, in the equivalent circuit, a constant phase element (CPE) is, generally, introduced to replace a true capacitor, to account for effects of roughness and other inhomogeneities of electrodes exactly and to determine the impedance parameters precisely.

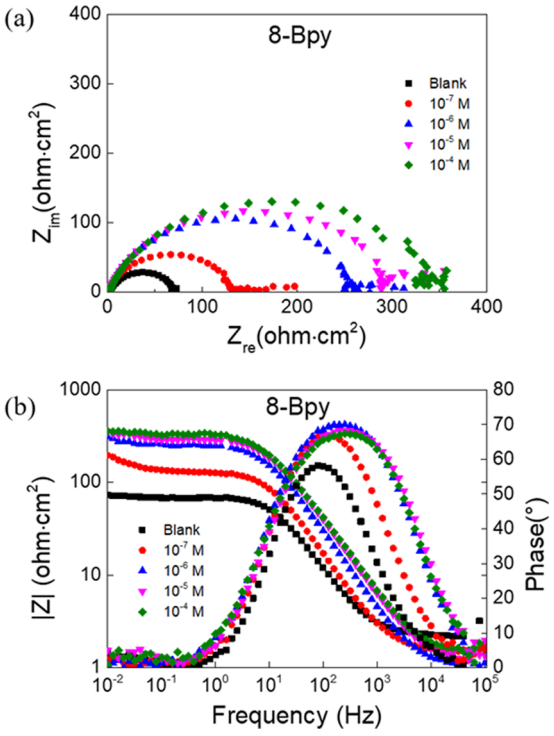

Figure 2. (a) Nyquist plots and (b) Bode plots for carbon steel in 1 M HCl containing different concentrations of 8-Bpy.

Figure 3 shows the corresponding equivalent circuit used to analyze the impedance data. Herein, the equivalent circuit consists of a serial connection between a solution resistance R_s and a parallel connection of a constant phase element (CPE) and a polarization resistance R_p, which contains the charge-transfer resistance R_{ct}, the resistance of diffusive layer R_d and inhibitor layer R_i, and the accumulated substances at the steel surface R_a, $R_p = R_{ct} + R_d + R_i + R_a$.[35,35] Figure 4 shows Nyquist plots (a) and Bode and phase angle plots (b) of 8-Bpy, which are perfectly fitted by the equivalent circuit used (those of 10-Bpy and 12-Bpy, see Figures S6 and S7). The impedance of CPE in the equivalent circuits is given by[36]

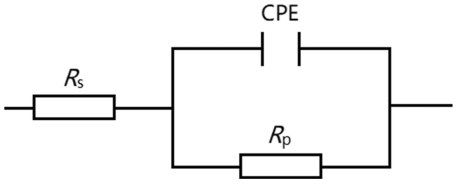

Figure 3. Electrochemical equivalent circuits used to fit the impedance data.

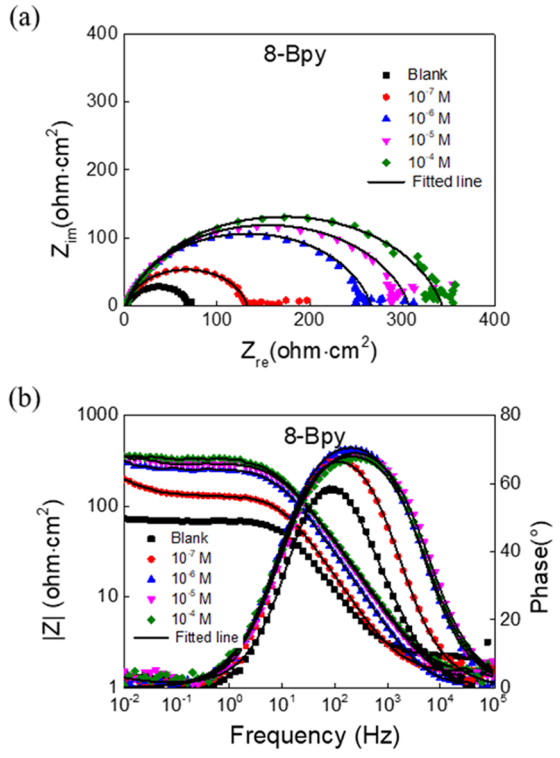

Figure 4. (a) Nyquist plots and (b) Bode plots of 8-Bpy fitted by the used equivalent circuits.

$$Z_{CPE} = \frac{1}{Y_0(j\omega)^n} \quad (5)$$

DOI: 10.1021/acsomega.8b03043
ACS Omega 2018, 3, 18990−18999

Table 3. EIS Parameters for Carbon Steel in 1 M HCl in the Absence and Presence of Different Concentrations of *n*-Bpys, and 10^{-5} M *n*-Bpys + 0.1 M KI

				CPE			
inhibitor	C_{inh}/M	R_s/Ω cm^2	R_p/Ω cm^2	Y_0/μS s^n cm^{-2}	n	C_{dl}/μF cm^{-2}	η/%
blank	0	2.235	68.05	330.2	0.8618	180.5	
8-Bpy	10^{-7}	1.532	131.1	208.4	0.8736	123.5	48.1
	10^{-6}	1.084	265.2	127.3	0.8613	74.02	74.3
	10^{-5}	1.250	306.2	107.9	0.8426	58.32	77.8
	10^{-4}	1.511	341.6	107.8	0.8357	56.71	80.1
8-Bpy + 0.1 M KI	10^{-5}	1.609	839.2	45.90	0.8872	30.31	91.9
10-Bpy	10^{-7}	1.435	143.3	209.9	0.8590	117.1	52.5
	10^{-6}	1.482	292.9	141.1	0.8509	81.52	76.8
	10^{-5}	1.923	325.4	125.6	0.8211	62.41	79.1
	10^{-4}	2.085	436.6	113.8	0.8223	59.18	84.4
10-Bpy + 0.1 M KI	10^{-5}	1.740	1092	54.30	0.8645	34.03	93.8
12-Bpy	10^{-7}	1.711	170.6	169.1	0.8447	88.90	60.1
	10^{-6}	1.567	293.4	138.3	0.8621	83.26	76.8
	10^{-5}	1.464	389.9	135.6	0.8165	69.03	82.5
	10^{-4}	1.508	393.8	129.6	0.8168	66.05	82.7
12-Bpy + 0.1 M KI	10^{-5}	1.988	882.7	40.70	0.8941	27.56	92.3

where Y_0 is the CPE constant, j is the imaginary unit, ω is the angular frequency, and n is the CPE exponent. Y_0 is converted into C_{dl} by the following expression[37]

$$C_{dl} = Y_0(\omega_{max})^{n-1} \quad (6)$$

where $\omega_{max} = 2\pi f_{max}$ represents the angular frequency at the maximum value of the imaginary part. The inhibition efficiency was calculated using the polarization resistance from the following equation

$$\eta = \frac{R_p - R_p^0}{R_p} \times 100\% \quad (7)$$

where R_p and R_p^0 are the polarization resistance values with and without *n*-Bpys, respectively. The impedance parameters derived from the equivalent circuit model are compiled in Table 3.

Polarization resistances R_p, closely associated with the inhibition efficiencies, in the presence of *n*-Bpys were always greater than their values in the absence of *n*-Bpys; moreover, their values increased as a function of *n*-Bpy concentrations. These results indicate a reduction in the steel corrosion rate when using *n*-Bpys as inhibitors. In contrast, the addition of *n*-Bpys results in an obvious decrease in C_{dl} values, which is a likely consequence of the adsorption of *n*-Bpy on the carbon steel surface.[38] In this regard, the adsorption of *n*-Bpys would lead to the increase of the adsorbed film thickness and/or the decrease in the local dielectric constant. The latter case was attributed to the fact that H_2O molecules on the electrode surface were gradually replaced by the adsorbed *n*-Bpy molecules with a lower dielectric constant.[39] Therefore, the variation in R_p and C_{dl} as a function of *n*-Bpy concentrations further confirms that *n*-Bpy molecules can form a protective layer via adsorbing at the metal/acid solution interface and prevent the metal surface against the attack of corrosive media.[11]

The Bode plots for carbon steel in 1 M HCl without and with 8-Bpy are given in Figure 2b. In Bode plots, the impedance values in the presence of 8-Bpy are higher than those in the absence of 8-Bpy, and they augment with the increasing concentration, further indicating the formation of a protective layer on the surface of carbon steel. By contrast, in phase angle plots, a single-phase peak reveals the presence of only one time constant in the presence of 8-Bpy, due to the formation of an electrical double layer at the solution/metal interface, and the angle increases after the addition of 8-Bpy.[40] Moreover, the phase angle values enhanced in the presence of *n*-Bpys, compared to those in the absence of *n*-Bpys, which manifests that the adsorption of *n*-Bpys molecules on the steel surface leads to greater smoothness of such surface.

Figure 5 shows the Nyquist plots and Bode plots of carbon steel in 1 M HCl containing 10^{-5} M 8-Bpy without and with 0.1 M KI (those of 10-Bpy and 12-Bpy, see Figures S8 and S9). Obviously, the addition of iodide ions results in a remarkable

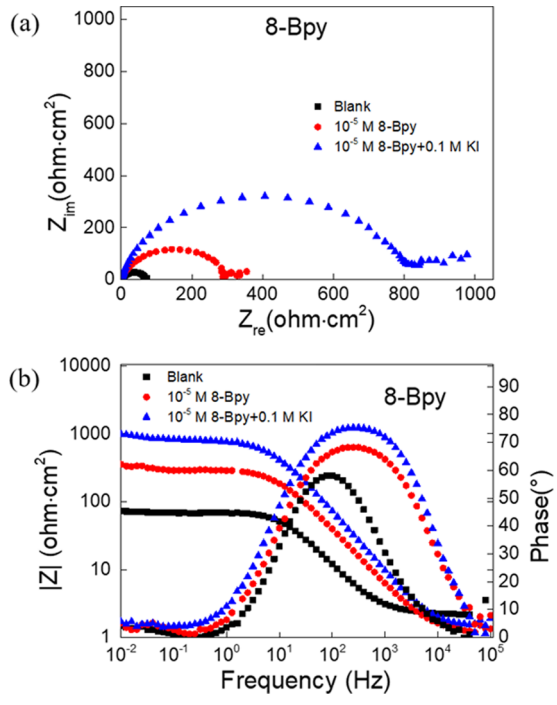

Figure 5. (a) Nyquist plots and (b) Bode plots for carbon steel in 1 M HCl of blank, blank + 10^{-5} M 8-Bpy and blank + 10^{-5} M 8-Bpy + 0.1 M KI.

DOI: 10.1021/acsomega.8b03043
ACS Omega 2018, 3, 18990−18999

increase in the diameters of the semicircles and the impedance values; meanwhile, in phase angle plots, a wider frequency region and a larger phase angle are displayed. All results in Figure 5 and Table 3 demonstrate that the presence of KI leads to a remarkable increase in the polarization resistance, R_p, but a reduced double-layer capacitance, C_{dl}. Similarly, these results may be ascribed to the adsorption of *n*-Bpys and I^- on the metal surface, leading to the formation of a protective film on the steel surface and in turn an enhanced corrosion inhibition. When the 1 M HCl solution only contains 10^{-5} M *n*-Bpy, the R_p values of 8, 10, and 12-Bpy were 306.2, 365.4, and 389.9 Ω cm^2, and the inhibition efficiencies were 77.8, 79.1, and 82.5%, respectively. However, the corresponding inhibition efficiencies increased up to 91.9, 93.8, and 92.3% after the addition of KI. These outcomes further indicate that iodide ions can improve the inhibition performance.

The inhibition efficiencies from EIS are in agreement with those obtained from the weight loss measurements and the potentiodynamic polarization methods, but with different absolute values. This is due to the differences in experimental methods, conditions, and the soaking time in aggressive media.

2.4. Adsorption Isotherm. The information of the interaction between the inhibitor molecules and the metal surface is generally provided by adsorption isotherms.[41] Assuming a direct relationship between the surface coverage (θ) and the inhibition efficiency (η) as $\theta = \eta/100$, weight loss measurements were used to determine the surface coverage values (θ) for *n*-Bpys in this work. Herein, the Langmuir adsorption isotherm model was employed to fit the results, given

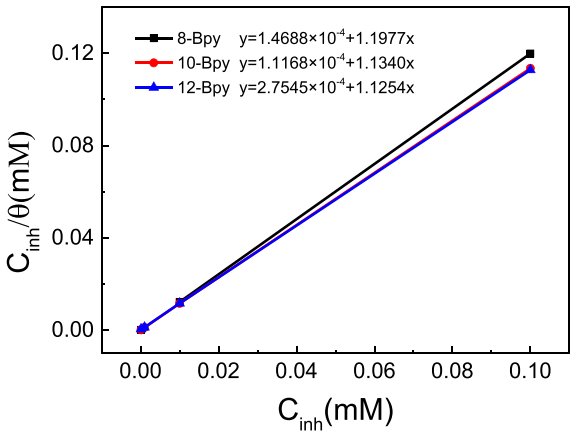

Figure 6. Langmuir adsorption isotherms for carbon steel in 1 M HCl of *n*-Bpys.

in Figure 6. In this model, θ is related to the concentration of the inhibitors (C_{inh}) by the following equation[42]

$$\frac{C_{inh}}{\theta} = \frac{1}{K_{ads}} + C_{inh} \quad (8)$$

where K_{ads} stands for the equilibrium constant in the adsorption process. The adsorption isotherms of *n*-Bpys in 1 M HCl have high correlation coefficients (R^2) of 0.9999, which is used as a measure to determine the best-fit adsorption isotherm. In this work, such high R^2 value indicates that the adsorption of *n*-Bpys on steel surface fully obeys Langmuir isothermal adsorption. Generally, the Langmuir isothermal adsorption postulates that no interactions occurred between the adjacent molecules adsorbed on the metal surface.[43] The equilibrium constant (K_{ads}) was obtained from the intercept of the Langmuir isotherm, given in Table 4. The equilibrium constant (K_{ads})

Table 4. Thermodynamic Parameters of Adsorption for Carbon Steel in 1 M HCl of *n*-Bpys

inhibitor	$K_{ads}/\times10^3$ L mol^{-1}	ΔG_{ads}/kJ mol^{-1}
8-Bpy	6808.28	−48.93
10-Bpy	8954.15	−49.61
12-Bpy	3630.42	−47.37

was used to determine the standard Gibbs free energy of the adsorption process using the following equation[44]

$$-\Delta G_{ads} = RT \ln(55.5K_{ads}) \quad (9)$$

where the value 55.5 represents the molar concentration of water in solution, R is the molar gas constant, and T is the absolute temperature. The calculated ΔG_{ads} values are also given in Table 4.

In general, the physisorption process is considered to associate with the electrostatic interaction between the charged corrosion inhibitor and the metal surface with the opposite charge, and the corresponding ΔG_{ads} values are usually less than −20 kJ mol^{-1}; in contrast, the chemisorption process is doomed to relate with the charge sharing or charge transfer from the inhibitor molecules to the metal surface, while the ΔG_{ads} values are commonly close to or more than −40 kJ mol^{-1}.[45] Here, the values of ΔG_{ads} were −48.93, −49.61, and −47.37 kJ mol^{-1} for 8-Bpy, 10-Bpy, and 12-Bpy, respectively. This suggests that *n*-Bpys can form a stable protection layer on carbon steel in 1 M HCl solution through a typical of chemisorption mechanism.[13]

2.5. Surface Characterization. SEM images and the corresponding EDS images of the freshly polished carbon steel specimen and those of carbon steel exposed to the uninhibited and inhibited 1 M HCl solution are shown in Figure 7. The EDS results were obtained from the whole surface of the corresponding SEM images. The SEM image of Figure 7b reveals a rougher surface for the uninhibited system, compared to that with the inhibited system (Figure 7c), which lends direct support to the anticorrosion effect of *n*-Bpys. Figure 7e denotes the EDS images of carbon steel corroded in 1 M HCl solution without any inhibitor, which describes lower characteristic signals of Fe, Mn, and Cr than those of polished carbon steel and shows the appearance of O element, which meant the presence of iron oxide. Furthermore, Fe peaks are considerably suppressed and Fe content is reduced from 93.53% (for carbon steel prior to immersion) to 73.83% (for carbon steel in 1 M HCl solution). These results suggested that the oxide film covered specimen surface. In the presence of 8-Bpy, the EDS images of Figure 7f show an additional peak of N indicating the adsorption of inhibitor molecules at the steel surface. Meanwhile, the mass ratio of Fe enhanced from 73.83 to 88.40%, while that of O dropped from 10.83 to 3.07%, compared to the specimen in 1 M HCl solution without 8-Bpy. These data indicated that inhibitors had absorbed on the surface, resulting in a reduction of the degree of acid corrosion.

2.6. Inhibition Mechanism of *n*-Bpy. Taken together, weight loss, electrochemical, isothermal adsorption, and morphological results suggest that the addition of *n*-Bpys plays a critical role in the corrosion inhibition of the carbon steel in 1 M HCl in this work. Based on such results and combined with the molecular structure of used *n*-Bpys, a schematic mechanism

DOI: 10.1021/acsomega.8b03043
ACS Omega 2018, 3, 18990−18999

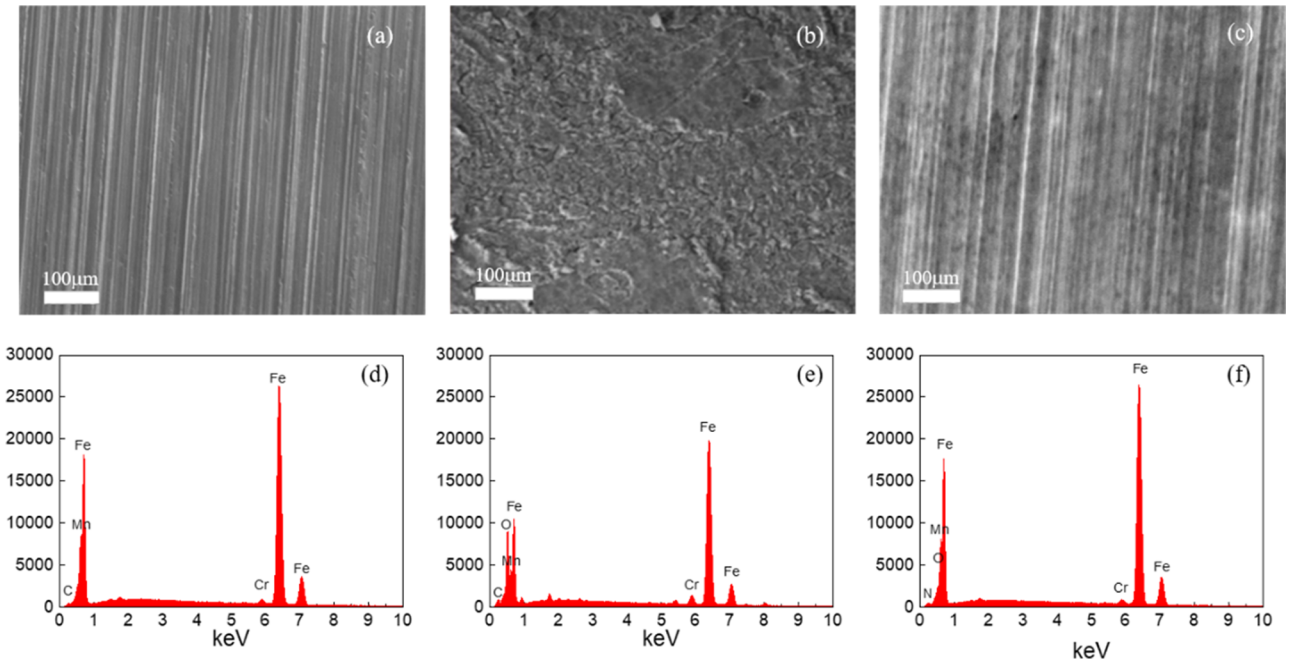

Figure 7. SEM images of carbon steel prior to immersion (a), after 48 h immersion in 1 M HCl solution without (b) and with (c) 10^{-4} M 8-Bpy and the corresponding EDS images of carbon steel prior to immersion (d), without (e) and with (f) 10^{-4} M 8-Bpy.

of the inhibition is proposed, shown in Chart 2. Since *n*-Bpys bear lone-pair electrons of the electronegative heteroatom N and

Chart 2. Schematic Representation of Possible Adsorption Interactions of *n*-Bpys on Carbon Steel Surface in HCl Solution

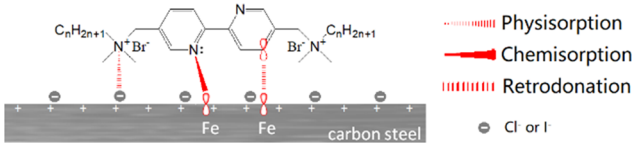

π-electrons of aromatic rings and iron atoms have vacant d-orbitals on the metal surface, which can mainly contribute to the chemisorption,[46] the coordinated interactions would be formed readily on the metal surface. This is in good agreement with the result of adsorption isotherms. It should be noted that the electrons may accumulate in d-orbitals of iron atoms, which is caused by the electron transfer during the chemisorption process and results in interelectronic repulsions on the metal surface. At this time, this repulsion could be abated by the reverse transfer of electrons from d-orbitals of iron atoms to the vacant antibonding molecular orbitals of *n*-Bpy molecules, known as retrodonation.[47] In this work, this case is illustrated in Chart 2. Last but not least, carbon steel is corroded in the aggressive solution, resulting in a positively charged metallic surface. Such a surface can attract the negatively charged counterions, such as chloride or iodide ions, thereby affording a net result being a negatively charged steel surface.[48] Accordingly, electrostatic interactions can also occur spontaneously between positively charged *n*-Bpy molecules and negatively charged metallic surface in acidic solution or in the presence of KI sometimes, which can be a contributor to the physisorption. As mentioned above, *n*-Bpys can play a key role in the corrosion inhibition of the carbon steel as mixed-type inhibitors with a predominant control of the cathodic reaction. The quaternary ammonium cation of *n*-Bpys may adsorb on the cathodic sites of carbon steel and inhibit the hydrogen evolution reaction, while N heteroatoms and aromatic rings may adsorb on anodic sites of metal surface and thus reduce the anodic metal dissolution reaction.[49]

One final point that deserves comment is a disagreement about the effect of the alkyl chain length or carbon atom numbers on the corrosion inhibition between the Gemini surfactants reported in other previous works[11,18,19] and *n*-Bpys used in this work, namely, that the anticorrosion performance of Gemini improves as their alkyl chain length is increased,[11,18,19] while *n*-Bpys do not exhibit this tendency. We believed that such a disagreement might be attributed to the orientation of adsorbed Gemini surfactant on the carbon steel surface, which can greatly affect the inhibition efficiency, as discussed elsewhere.[21] However, the bipyridyl spacer is a rigid group. As discussed in our previous work,[50,51] it is the rigid spacer that forces the two alkyl chains to separate, thereby almost producing a fully extended configuration lie nearly flat on the water surface; and only when the surface pressure is sufficiently enough, i.e., more than 30 mN m^{-1}, it is possible to partially reorient both horizontal chains into a vertical arrangement. Such a fully extended configuration of Geminis with a rigid spacer was also evidenced by the crystallographic data[52−54] from single-crystal X-ray diffraction and the molecular arrangement at the air/water interface from the polarization modulation infrared reflection-absorption spectroscopy (PM-IRRAS)[55] in our previous work. Especially, in the latter case, PM-IRRAS revealed that the tilt angles of chains with respect to the surface normal were in the range of 73−76°. Herein, *n*-Bpys have a rigid bipyridyl spacer, which may adsorb in a similarly extended mode on the steel surface (for more details, see the analysis for π−*A* isotherm of 18-Bpy in Figures S10 and S11), in contrast to other Geminis whose alkyl chains are pending from the metal surface and pointing toward the aggressive media almost perpendicularly. Therefore, the fact that the variation in the alkyl chain length of *n*-Bpys has a negligible effect on the anticorrosion performance in this work may be attributed to the unique molecular

DOI: 10.1021/acsomega.8b03043
ACS Omega 2018, 3, 18990−18999

configuration. Herein, the CMC value of 8-Bpy, as a representative species, was determined to be 2.22 mM, based on the surface tension measurement (see Figure S12). Furthermore, such a simple model can also account for the differences in the inhibition efficiency between Geminis previously reported in other work and *n*-Bpys in this work, at extremely low and medium concentrations, respectively (here, this comparison was not conducted at high concentrations due to the solubility limitation of *n*-Bpys). At extremely low concentrations, e.g., 10^{-6} M, inhibition efficiencies of *n*-Bpys nearly exceed 75%, superior to those of the other Geminis reported previously, while at medium concentrations, e.g., 10^{-4} M, they are almost more than 80%, comparable to the other values.[25,29,30] This is a likely consequence of *n*-Bpys having multiple interactions with the steel surface, which is helpful for a facile and rapid adsorption with a relatively larger surface coverage at extremely low concentrations and the formation of a tightly adsorbed layer, thereby facilitating an improved inhibition efficiency.

3. CONCLUSIONS

In this work, *n*-Bpys simultaneously bearing three functional groups, i.e., heteroatoms, aromatic rings, and quaternary ammonium head, have been successfully prepared and explored the inhibition performance for carbon steel in 1 M HCl solution. Several results of *n*-Bpys are listed below:

1. *n*-Bpys effectively act as corrosion inhibitors for carbon steel in 1 M HCl solution at low concentrations, and the inhibition efficiency improved with increasing concentration of *n*-Bpys. Moreover, the addition of the iodide ions can dramatically improve their inhibitive performances.
2. Potentiodynamic polarization curves indicated that *n*-Bpys were a mixed-type inhibitor with a predominantly cathodic control.
3. EIS measurements showed that a protective layer was formed on the carbon steel surface according to the decrease of the C_{dl} value and the increase of the R_p with increasing inhibitor concentration.
4. Adsorption of *n*-Bpys on the carbon steel surface obeyed the Langmuir isotherm. The values of ΔG_{ads} are −48.93, −49.61, and −47.37 kJ mol^{-1} for 8-Bpy, 10-Bpy, and 12-Bpy, respectively, which indicate that the adsorption of *n*-Bpys is a typical chemisorption process.
5. SEM/EDAX images revealed a smoother carbon steel surface in inhibited acid solution compared to that in the uninhibited system, which suggests that a protective film was formed on the metal surface.
6. The carbon chain length of *n*-Bpys played a negligible role in the inhibition efficiency due to the orientation of the tail chain of the molecule.

Efforts aimed at exploring the contribution degree of each functional group to the corrosion inhibition, with a view toward creating high-efficiency inhibitors, are continuing in our lab.

4. EXPERIMENTAL SECTION

4.1. Synthesis of Inhibitors. The inhibitors used in this work were obtained using experimental procedures similar to those described in our previous work.[53,54] In brief, an intermediate, 5,5′-bis(bromomethyl)-2,2′-bipyridine, was obtained from a bromination reaction of 5,5′-dimethyl-2,2′-bipyridine. Subsequently, a quaterization reaction of 5,5′-*N*,*N*-dimethyloctylamine with bis(bromomethyl)-2,2′-bipyridine afforded 8-Bpy. In the same way, 10-Bpy and 12-Bpy were synthesized via the quaterization reaction of *N*,*N*-dimethyldecylamine and *N*,*N*-dimethyldodecylamine with 5,5′-bis(bromomethyl)-2,2′-bipyridine, respectively.

4.2. Materials and Solutions. The composition of tested specimen of N80 is (wt %): C: 0.35; Si: 0.23; Mn: 1.46; P: 0.011; S: 0.005; Cu: 0.08; Ni: 0.01; Cr: 0.08; Mo: 0.16; V: 0.11; Al: 0.024; Fe balance. Prior to the experiment, the specimen was washed ultrasonically with ultrapure water, alcohol, and acetone and finally dried in air.

The simulated corrosion solution of 1 M HCl was prepared by an analytically pure concentrated hydrochloric acid in a mass fraction of 36−38% (analytically pure), which was also used as a blank sample for comparison. The concentration range of *n*-Bpys used for corrosion measurements from 10^{-7} to 10^{-4} M. All tests were carried out at 298 ± 1 K.

4.3. Weight Loss Measurement. The dimension of used carbon steel specimens was 5 cm × 1 cm × 0.3 cm. All samples were immersed in 1 M HCl solution in the absence and presence of different concentrations of *n*-Bpys for 48 h. Each condition was repeated at least three times, and the mean weight losses were reported.

4.4. Electrochemical Measurements. Electrochemical tests were carried out by a conventional three-electrode system, assembled with carbon steel sheet as the working electrode, a platinum wire as the counter electrode, and Ag/AgCl (3.5 M KCl) as the reference electrode, on a PARSTAT4000 electrochemical workstation (Princeton Applied Research). A carbon steel sheet was pressed to fit into a poly(tetrafluoroethylene) holder, while exposing only 2.9 cm^2 surface to the solution.

Polarization experiments were performed in the potential range of ±0.25 V versus the open-circuit potential with a scan rate of 0.5 mV s^{-1}. In the electrochemical impedance spectroscopy (EIS) measurements, the frequency range is from 100 kHz to 10 mHz by applying 5 mV amplitude to the system. The EIS data were fitted and processed carefully by ZSimpWin software. It should be noted that prior to each experiment, the working electrode was immersed in the test solution for 30 min to measure the open-circuit potential and all experiments were repeated at least three times.

4.5. Surface Characterization. For surface morphological investigations of the carbon steel samples in the absence and presence of *n*-Bpys, scanning electron microscopy (SEM) and energy-dispersive spectrometry (EDS) were performed using FEI Nova Nano SEM with TEAM EDS. The specimens with size of 1 cm × 1 cm × 0.1 cm were prepared. After the immersion in 1 M HCl solution without and with 10^{-4} M 8-Bpy for 48 h, the specimens were thoroughly rinsed with distilled water, dried, and subjected to SEM/EDS analysis.

■ ASSOCIATED CONTENT

Supporting Information

The Supporting Information is available free of charge on the ACS Publications website at DOI: 10.1021/acsomega.8b03043.

Effect of temperature on the corrosion inhibition efficiency of 12-Bpy; potentiodynamic polarization curves for carbon steel in 1 M HCl without and with different concentrations of 10-Bpy and 12-Bpy; potentiodynamic polarization curves for carbon steel in 1 M HCl + 10^{-5} M 10-Bpy and 12-Bpy in the absence and presence of 0.1 M KI; Nyquist and Bode plots for carbon steel in 1 M HCl

DOI: 10.1021/acsomega.8b03043
ACS Omega 2018, 3, 18990−18999

containing different concentrations of 10-Bpy and 12-Bpy; Nyquist plots and Bode plots of 10-Bpy and 12-Bpy fitted by the used equivalent circuits; Nyquist plots and Bode plots for carbon steel in 1 M HCl of blank, blank + 10^{-5} M 10-Bpy and blank + 10^{-5} M 10-Bpy + 0.1 M KI; Nyquist plots and Bode plots for carbon steel in 1 M HCl of blank, blank + 10^{-5} M 12-Bpy and blank + 10^{-5} M 12-Bpy + 0.1 M KI; surface pressure−molecular area isotherms of 18-Bpy and the analysis of the chain orientation; surface tension of 8-Bpy at different concentrations at 298 K (PDF)

AUTHOR INFORMATION

Corresponding Authors

*E-mail: yincx@cnpc.com.cn (C.Y.).
*E-mail: qibinchen@ecust.edu.cn (Q.C.).

ORCID

Qibin Chen: 0000-0002-1095-1307
Honglai Liu: 0000-0002-5682-2295

Notes

The authors declare no competing financial interest.

ACKNOWLEDGMENTS

This work was funded by Open Foundation of The State Key Laboratory for Performance and Structure Safety of Petroleum Tubular Goods and Equipment Materials (2017-FW-76), the National Natural Science Foundation of China (Nos. 21576079, 91334203), the 111 Project of Ministry of Education of China (No. B08021), and the Fundamental Research Funds for the Central Universities of China.

REFERENCES

(1) Kumar, S.; Vashisht, H.; Olasunkanmi, L. O.; Bahadur, I.; Verma, H.; Goyal, M.; Singh, G.; Ebenso, E. E. Polyurethane Based Triblock Copolymers as Corrosion Inhibitors for Mild Steel in 0.5 M H_2SO_4. *Ind. Eng. Chem. Res.* **2017**, *56*, 441−456.

(2) Odewunmi, N. A.; Umoren, S. A.; Gasem, Z. M. Watermelon waste products as green corrosion inhibitors for mild steel in HCl solution. *J. Environ. Chem. Eng.* **2015**, *3*, 286−296.

(3) Kaczerewska, O.; Leiva-Garcia, R.; Akid, R.; Brycki, B.; Kowalczyk, I.; Pospieszny, T. Effectiveness of O-bridged cationic gemini surfactants as corrosion inhibitors for stainless steel in 3 M HCl: Experimental and theoretical studies. *J. Mol. Liq.* **2018**, *249*, 1113−1124.

(4) Prabhu, R. A.; Venkatesha, T. V.; Shanbhag, A. V.; Praveen, B. M.; Kulkarni, G. M.; Kalkhambkar, R. G. Quinol-2-thione compounds as corrosion inhibitors for mild steel in acid solution. *Mater. Chem. Phys.* **2008**, *108*, 283−289.

(5) Mobin, M.; Aslam, R.; Aslam, J. Non toxic biodegradable cationic gemini surfactants as novel corrosion inhibitor for mild steel in hydrochloric acid medium and synergistic effect of sodium salicylate: Experimental and theoretical approach. *Mater. Chem. Phys.* **2017**, *191*, 151−167.

(6) Moretti, G.; Guidi, F.; Fabris, F. Corrosion inhibition of the mild steel in 0.5M HCl by 2-butyl-hexahydropyrrolo[1,2-b][1,2]oxazole. *Corros. Sci.* **2013**, *76*, 206−218.

(7) Faustin, M.; Maciuk, A.; Salvin, P.; Roos, C.; Lebrini, M. Corrosion inhibition of C38 steel by alkaloids extract of *Geissospermum laeve* in 1M hydrochloric acid: Electrochemical and phytochemical studies. *Corros. Sci.* **2015**, *92*, 287−300.

(8) El Hamdani, N.; Fdil, R.; Tourabi, M.; Jama, C.; Bentiss, F. Alkaloids extract of *Retama monosperma* (L.) Boiss. seeds used as novel eco-friendly inhibitor for carbon steel corrosion in 1 M HCl solution: Electrochemical and surface studies. *Appl. Surf. Sci.* **2015**, *357*, 1294−1305.

(9) Negm, N. A.; Ghuiba, F. M.; Tawfik, S. M. Novel isoxazolium cationic Schiff base compounds as corrosion inhibitors for carbon steel in hydrochloric acid. *Corros. Sci.* **2011**, *53*, 3566−3575.

(10) Behpour, M.; Ghoreishi, S. M.; Soltani, N.; Salavati-Niasari, M.; Hamadanian, M.; Gandomi, A. Electrochemical and theoretical investigation on the corrosion inhibition of mild steel by thiosalicylaldehyde derivatives in hydrochloric acid solution. *Corros. Sci.* **2008**, *50*, 2172−2181.

(11) Abd El-Lateef, H. M.; Abo-Riya, M. A.; Tantawy, A. H. Empirical and quantum chemical studies on the corrosion inhibition performance of some novel synthesized cationic gemini surfactants on carbon steel pipelines in acid pickling processes. *Corros. Sci.* **2016**, *108*, 94−110.

(12) Tawfik, S. M. Corrosion inhibition efficiency and adsorption behavior of N,N-dimethyl-4-(((1-methyl-2-phenyl-2,3-dihydro-1H-pyrazol-4-yl)imino)methyl)-N-alkylbenzenaminium bromide surfactant at carbon steel/hydrochloric acid interface. *J. Mol. Liq.* **2015**, *207*, 185−194.

(13) Abd El-Lateef, H. M.; Soliman, K. A.; Tantawy, A. H. Novel synthesized Schiff Base-based cationic gemini surfactants: Electrochemical investigation, theoretical modeling and applicability as biodegradable inhibitors for mild steel against acidic corrosion. *J. Mol. Liq.* **2017**, *232*, 478−498.

(14) Migahed, M. A.; Shaban, M. M.; Fadda, A. A.; Ali, T. A.; Negm, N. A. Synthesis of some quaternary ammonium gemini surfactants and evaluation of their performance as corrosion inhibitors for carbon steel in oil well formation water containing sulfide ions. *RSC Adv.* **2015**, *5*, 104480−104492.

(15) Menger, F. M.; Keiper, J. S. Gemini surfactants. *Angew. Chem., Int. Ed.* **2000**, *39*, 1906−1920.

(16) Zana, R. Dimeric and oligomeric surfactants. Behavior at interfaces and in aqueous solution: a review. *Adv. Colloid Interface Sci.* **2002**, *97*, 205−253.

(17) Heakal, F. E.-T.; Elkholy, A. E. Gemini surfactants as corrosion inhibitors for carbon steel. *J. Mol. Liq.* **2017**, *230*, 395−407.

(18) Hegazy, M. A.; Abdallah, M.; Ahmed, H. Novel cationic gemini surfactants as corrosion inhibitors for carbon steel pipelines. *Corros. Sci.* **2010**, *52*, 2897−2904.

(19) Qiang, Y.; Zhang, S.; Guo, L.; Zheng, X.; Xiang, B.; Chen, S. Experimental and theoretical studies of four allyl imidazolium-based ionic liquids as green inhibitors for copper corrosion in sulfuric acid. *Corros. Sci.* **2017**, *119*, 68−78.

(20) El Achouri, M.; Kertit, S.; Gouttaya, H. M.; Nciri, B.; Bensouda, Y.; Perez, L.; Infante, M. R.; Elkacemi, K. Corrosion inhibition of iron in 1 M HCl by some gemini surfactants in the series of alkanediyl-α,ω-bis-(dimethyl tetradecyl ammonium bromide). *Prog. Org. Coat.* **2001**, *43*, 267−273.

(21) El Achouri, M.; Infante, M. R.; Izquierdo, F.; Kertit, S.; Gouttaya, H. M.; Nciri, B. Synthesis of some cationic gemini surfactants and their inhibitive effect on iron corrosion in hydrochloric acid medium. *Corros. Sci.* **2001**, *43*, 19−35.

(22) Hegazy, M. A.; Rashwan, S. M.; Kamel, M. M.; El Kotb, M. S. Synthesis, surface properties and inhibition behavior of novel cationic gemini surfactant for corrosion of carbon steel tubes in acidic solution. *J. Mol. Liq.* **2015**, *211*, 126−134.

(23) Tawfik, S. M.; Abd-Elaal, A. A.; Aiad, I. Three gemini cationic surfactants as biodegradable corrosion inhibitors for carbon steel in HCl solution. *Res. Chem. Intermed.* **2016**, *42*, 1101−1123.

(24) Tawfik, S. M. Ionic liquids based gemini cationic surfactants as corrosion inhibitors for carbon steel in hydrochloric acid solution. *J. Mol. Liq.* **2016**, *216*, 624−635.

(25) Hegazy, M. A. A novel Schiff base-based cationic gemini surfactants: Synthesis and effect on corrosion inhibition of carbon steel in hydrochloric acid solution. *Corros. Sci.* **2009**, *51*, 2610−2618.

(26) Umoren, S. A.; Solomon, M. M. Effect of halide ions on the corrosion inhibition efficiency of different organic species − A review. *J. Ind. Eng. Chem.* **2015**, *21*, 81−100.

(27) Fouda, A. S.; Mostafa, H. A.; El-Taib, F.; Elewady, G. Y. Synergistic influence of iodide ions on the inhibition of corrosion of C-

DOI: 10.1021/acsomega.8b03043
ACS Omega 2018, 3, 18990−18999

steel in sulphuric acid by some aliphatic amines. *Corros. Sci.* **2005**, *47*, 1988−2004.
(28) Jeyaprabha, C.; Sathiyanarayanan, S.; Venkatachari, G. Influence of halide ions on the adsorption of diphenylamine on iron in 0.5 M H_2SO_4 solutions. *Electrochim. Acta* **2006**, *51*, 4080−4088.
(29) Hegazy, M. A.; El-Tabei, A. S.; Bedair, A. H.; Sadeq, M. A. Synthesis and inhibitive performance of novel cationic and gemini surfactants on carbon steel corrosion in 0.5 M H_2SO_4 solution. *RSC Adv.* **2015**, *5*, 64633−64650.
(30) El Achouri, M.; Infante, M. R.; Izquierdo, F.; Kertit, S.; Gouttaya, H. M.; Nciri, B. Synthesis of some cationic gemini surfactants and their inhibitive effect on iron corrosion in hydrochloric acid medium. *Corros. Sci.* **2001**, *43*, 19−35.
(31) Fitoz, A.; Nazır, H.; Özgür; Emregül, E.; Emregul, K. An experimental and theoretical approach towards understanding the inhibitive behavior of a nitrile substituted coumarin compound as an effective acidic media inhibitor. *Corros. Sci.* **2018**, *133*, 451−464.
(32) Bobina, M.; Kellenberger, A.; Millet, J.-P.; Muntean, C.; Vaszilcsin, N. Corrosion resistance of carbon steel in weak acid solutions in the presence of L-histidine as corrosion inhibitor. *Corros. Sci.* **2013**, *69*, 389−395.
(33) Aslam, R.; Mobin, M.; Zehra, S.; Obot, I. B.; Ebenso, E. E. N,N′-Dialkylcystine Gemini and Monomeric N-Alkyl Cysteine Surfactants as Corrosion Inhibitors on Mild Steel Corrosion in 1 M HCl Solution: A Comparative Study. *ACS Omega* **2017**, *2*, 5691−5707.
(34) Yohai, L.; Vázquez, M.; Valcarce, M. B. Phosphate ions as corrosion inhibitors for reinforcement steel in chloride-rich environments. *Electrochim. Acta* **2013**, *102*, 88−96.
(35) El-Lateef, H. M. A.; Ahmed, H. T. Synthesis and evaluation of novel series of Schiff base cationic surfactants as corrosion inhibitors for carbon steel in acidic/chloride media: experimental and theoretical investigations. *RSC Adv.* **2016**, *6*, 8681−8700.
(36) Naderi, E.; Ehteshamzadeh, M.; Jafari, A. H.; Hosseini, M. G. Effect of carbon steel microstructure and molecular structure of two new Schiff base compounds on inhibition performance in 1 M HCl solution by DC, SEM and XRD studies. *Mater. Chem. Phys.* **2010**, *120*, 134−141.
(37) Torres, V. V.; Rayol, V. A.; Magalhães, M.; Viana, G. M.; Aguiar, L. C. S.; Machado, S. P.; Orofino, H.; D'Elia, E. Study of thioureas derivatives synthesized from a green route as corrosion inhibitors for mild steel in HCl solution. *Corros. Sci.* **2014**, *79*, 108−118.
(38) Quraishi, M. A.; Rawat, J. Influence of iodide ions on inhibitive performance of tetraphenyl-dithia-octaaza-cyclotetradeca-hexaene (PTAT) during pickling of mild steel in hot sulfuric acid. *Mater. Chem. Phys.* **2001**, *70*, 95−99.
(39) Ghanbari, A.; Attar, M. M.; Mahdavian, M. Corrosion inhibition performance of three imidazole derivatives on mild steel in 1 M phosphoric acid. *Mater. Chem. Phys.* **2010**, *124*, 1205−1209.
(40) Sığırcık, G.; Tüken, T.; Erbil, M. Assessment of the inhibition efficiency of 3,4-diaminobenzonitrile against the corrosion of steel. *Corros. Sci.* **2016**, *102*, 437−445.
(41) Zarrouk, A.; Hammouti, B.; Lakhlifi, T.; Traisnel, M.; Vezin, H.; Bentiss, F. New 1H-pyrrole-2,5-dione derivatives as efficient organic inhibitors of carbon steel corrosion in hydrochloric acid medium: Electrochemical, XPS and DFT studies. *Corros. Sci.* **2015**, *90*, 572−584.
(42) Deng, S.; Li, X.; Fu, H. Acid violet 6B as a novel corrosion inhibitor for cold rolled steel in hydrochloric acid solution. *Corros. Sci.* **2011**, *53*, 760−768.
(43) Obot, I. B.; Obi-Egbedi, N. O.; Umoren, S. A. Antifungal drugs as corrosion inhibitors for aluminium in 0.1M HCl. *Corros. Sci.* **2009**, *51*, 1868−1875.
(44) Hegazy, M. A.; Zaky, M. F. Inhibition effect of novel nonionic surfactants on the corrosion of carbon steel in acidic medium. *Corros. Sci.* **2010**, *52*, 1333−1341.
(45) Okafor, P. C.; Zheng, Y. Synergistic inhibition behaviour of methylbenzyl quaternary imidazoline derivative and iodide ions on mild steel in H_2SO_4 solutions. *Corros. Sci.* **2009**, *51*, 850−859.
(46) Verma, C.; Quraishi, M. A.; Singh, A. A thermodynamical, electrochemical, theoretical and surface investigation of diheteroaryl thioethers as effective corrosion inhibitors for mild steel in 1 M HCl. *J. Taiwan Inst. Chem. Eng.* **2016**, *58*, 127−140.
(47) Roy, P.; Karfa, P.; Adhikari, U.; Sukul, D. Corrosion inhibition of mild steel in acidic medium by polyacrylamide grafted Guar gum with various grafting percentage: Effect of intramolecular synergism. *Corros. Sci.* **2014**, *88*, 246−253.
(48) Goyal, M.; Kumar, S.; Bahadur, I.; Verma, C.; Ebenso, E. E. Organic corrosion inhibitors for industrial cleaning of ferrous and non-ferrous metals in acidic solutions: A review. *J. Mol. Liq.* **2018**, *256*, 565−573.
(49) Zou, C.; Yan, X.; Qin, Y.; Wang, M.; Liu, Y. Inhibiting evaluation of *β*-Cyclodextrin-modified acrylamide polymer on alloy steel in sulfuric solution. *Corros. Sci.* **2014**, *85*, 445−454.
(50) Qibin, C.; Liang, X. D.; Wang, S. L.; Xu, S. H.; Liu, H. L.; Hu, Y. Cationic Gemini surfactant at the air/water interface. *J. Colloid Interface Sci.* **2007**, *314*, 651−658.
(51) Chen, Q. B.; Zhang, D. Z.; Li, R.; Liu, H. L.; Hu, Y. Effect of the spacer group on the behavior of the cationic Gemini surfactant monolayer at the air/water interface. *Thin Solid Films* **2008**, *516*, 8782−8787.
(52) Sheng, Y. J.; Yao, J. Y.; Chen, Q. B.; Liu, H. L. Effect of 1D twisted water chains confined in channels formed by a Gemini amphiphile on its crystal stability. *CrystEngComm* **2015**, *17*, 1439−1447.
(53) Yao, J. Y.; Chen, Q. B.; Sheng, Y. J.; Kai, A. T.; Liu, H. L. Reversible water uptake by a porous molecular crystal from metal complex of gemini surfactant. *CrystEngComm* **2017**, *19*, 802−810.
(54) Yao, J. Y.; Chen, Q. B.; Sheng, Y. J.; Kai, A. T.; Liu, H. L. pH-controlled crystal growth of copper/gemini surfactant complexes with bipyridine groups. *CrystEngComm* **2017**, *19*, 5835−5843.
(55) Chen, Q. B.; Yao, J. Y.; Hu, X.; Shen, J. C.; Sheng, Y. J.; Liu, H. L. Monolayer effect of a gemini surfactant with a rigid biphenyl spacer on its self-crystallization at the air/liquid interface. *J. Appl. Crystallogr.* **2015**, *48*, 728−735.

DOI: 10.1021/acsomega.8b03043
ACS Omega 2018, 3, 18990−18999